.
SCUOLA INTERNAZIONALE SUPERIORE DI STUDI AVANZATI

SISSA Digital Library

The final spin from binary black holes in quasi-circular orbits

Original
The final spin from binary black holes in quasi-circular orbits / Hofmann, F; Barausse, E; Rezzolla, L. - In: THE ASTROPHYSICAL JOURNAL LETTERS. - ISSN 2041-8205. - 825:2(2016), pp. 1-6.

Availability:
This version is available at: 20.500.11767/89695 since: 2019-04-18T11:52:19Z

Publisher:

Published
DOI:10.3847/2041-8205/825/2/L19

(Article begins on next page)

09 March 2020

THE FINAL SPIN FROM BINARY BLACK HOLES IN QUASI-CIRCULAR ORBITS

FABIAN HOFMANN[1], ENRICO BARAUSSE[2,3], LUCIANO REZZOLLA[1,4]

Draft version June 8, 2016

ABSTRACT

We revisit the problem of predicting the spin magnitude and direction of the black hole resulting from the merger of two black holes with arbitrary masses and spins inspiralling in quasi-circular orbits. We do this by analyzing a catalog of 619 recent numerical-relativity simulations collected from the literature and spanning a large variety of initial conditions. By combining information from the post-Newtonian approximation, the extreme mass-ratio limit and perturbative calculations, we improve our previously proposed phenomenological formulae for the final remnant spin. In contrast with alternative suggestions in the literature, and in analogy with our previous expressions, the new formula is a simple algebraic function of the initial system parameters and is not restricted to binaries with spins aligned/anti-aligned with the orbital angular momentum, but can be employed for fully generic binaries. The accuracy of the new expression is significantly improved, especially for almost extremal progenitor spins and for small mass ratios, yielding a root-mean-square error $\sigma \approx 0.002$ for aligned/anti-aligned binaries and $\sigma \approx 0.006$ for generic binaries. Our new formula is suitable for cosmological applications and can be employed robustly in the analysis of the gravitational waveforms from advanced interferometric detectors.

Subject headings: black hole physics, gravitational waves, gravitation

1. INTRODUCTION

According to the predictions of general relativity, binary systems of compact objects are the most efficient emitters of gravitational waves (GWs). Indeed, Advanced LIGO has recently detected the GW signal from a black-hole (BH) binary with masses $M_1 \approx 36\,M_\odot$ and $M_2 \approx 29\,M_\odot$ (Abbott et al. 2016), at a (luminosity) distance of ~ 410 Mpc. In general, Advanced LIGO and other terrestrial interferometers, such as Advanced Virgo and KAGRA, target BH binaries with a variety of masses (up to a few hundred $M_\odot$, if they exist; Belczynski et al. 2014, 2016). More massive BH binaries are targeted by existing pulsar-timing arrays (in the mass range $10^8 - 10^{10}\,M_\odot$; Manchester & IPTA 2013) and by future space-borne interferometers such as eLISA (in the mass range $10^4 - 10^7\,M_\odot$; Klein et al. 2016).

One of the obvious difficulties of observing BH binaries with terrestrial interferometers is that only the final part of the inspiral and the merger/ringdown are in band. This is where the perturbative post-Newtonian (PN) techniques valid earlier in the inspiral become inaccurate, preventing the extraction the source's physical parameters. Hence, to obtain the full gravitational waveforms, it is necessary to resort to numerical-relativity (NR) simulations. In practice, even under the reasonable assumption that BH binaries near the merger have been circularized by earlier GW emission, the space of parameters to be probed (the mass ratio q and the spin vectors $\boldsymbol{S}_1,\ \boldsymbol{S}_2$, *i.e.,* seven parameters) is too large to be handled by NR simulations alone.

To ensure a sufficient coverage of the parameter space, semi-analytical techniques allowing faster waveform production are employed, *e.g.,* the spin-effective-one-body (sEOB) model (Buonanno & Damour 1999; Damour 2001; Barausse & Buonanno 2010) or "hybrid" waveforms (Ajith et al. 2008; Khan et al. 2015), which combine results from NR simulations with PN and quasinormal-mode calculations. These techniques are faster, but require great care when modeling the merger and the transition to the ringdown. Indeed, although the ringdown can be modeled via a linear superposition of quasi-normal modes, their frequencies depend on the remnant BH's mass and spin, which, in turn, depend on the initial binary parameters.

This relation between the binary's initial and final states is highly non-trivial because it encodes the details of the strong-field, highly relativistic merger, which is only accessible via NR calculations. Yet, a number of approaches to predict analytically or semi-analytically the remnant's final spin magnitude and direction have been proposed. These range from modeling the GW fluxes throughout the binary's evolution within the EOB model (*e.g.,* by Damour & Nagar 2007, for nonspinning BHs) to approaches that combine information from PN theory, the extreme mass-ratio limit (EMRL), symmetry arguments, and fits to NR data, to provide "formulae" for the final spin (Rezzolla et al. 2008a; Kesden 2008; Rezzolla et al. 2008b; Tichy & Marronetti 2008; Rezzolla et al. 2008c; Buonanno et al. 2008; Barausse & Rezzolla 2009; Healy et al. 2014). Similar formulae have also been derived for the remnant's final mass (Tichy & Marronetti 2008; Kesden 2008; Barausse et al. 2012; Healy et al. 2014), which differs from the binary's total mass by the energy emitted in GWs. Again, a common problem in these attempts is the difficulty to cover with sufficient accuracy the seven-dimensional parameter space of quasi-circular BH binaries. Indeed, while most of these formulae formally cover the whole parameter space, they can be rather inaccurate, especially for BHs with almost extremal spins.

By combining results from NR and information from the EMRL and PN theory, we here derive a new formula for the spin magnitude and direction for the merger remnant from

[1] Institute for Theoretical Physics, Max-von-Laue-Str. 1, 60438 Frankfurt, Germany

[2] Sorbonne Universités, UPMC Univ Paris 06, UMR 7095, Institut d'Astrophysique de Paris, F-75014, Paris, France

[3] CNRS, UMR 7095, Institut d'Astrophysique de Paris, F-75014, Paris, France

[4] Frankfurt Institute for Advanced Studies, Ruth-Moufang-Str. 1, 60438 Frankfurt, Germany

quasi-circular BH binaries with arbitrary masses and spins. We calibrate our formula against a catalog of 619 recently published NR simulations (Chu et al. 2009; Hannam et al. 2010; Nakano et al. 2011; Sperhake et al. 2011; Pollney & Reisswig 2011; Kelly et al. 2011; Buchman et al. 2012; Lovelace et al. 2012; Hemberger et al. 2013; Hinder et al. 2013; Kelly & Baker 2013; Pekowsky et al. 2013; Healy et al. 2014; Lousto & Zlochower 2014; Lovelace et al. 2015; Scheel et al. 2015; Szilágyi et al. 2015; Zlochower & Lousto 2015; Husa et al 2016; SXS collaboration 2016)[5], and validate it by comparing its results to self-force calculations and plunge-merger-ringdown fluxes for nonspinning binaries with small mass ratios, as well as to a set of 248 NR simulations not included in the calibration dataset (Karan et al. 2016).

Our new formula builds upon Barausse & Rezzolla (2009), who introduced a final-spin formula that is widely used both in the production of semi-analytical waveforms (*e.g.,* in sEOB and phenomenological waveforms) and in cosmological studies of massive BH evolution (see, *e.g.,* Berti & Volonteri 2008; Fanidakis et al. 2011; Barausse 2012; Volonteri et al. 2013; Dubois et al. 2014; Sesana et al. 2014). Our novel prescription especially improves the accuracy of the formula by Barausse & Rezzolla (2009) for extreme mass ratios and for near-extremal spins. This is important since near-extremal spins are expected, at least in some cases, for supermassive BHs (Berti & Volonteri 2008; Fanidakis et al. 2011; Barausse 2012; Volonteri et al. 2013; Dubois et al. 2014; Sesana et al. 2014) and possibly also for stellar-mass BHs (McClintock et al. 2011). We assume $G = 1 = c$ hereafter.

2. MODELING THE FINAL SPIN

Let us first consider a BH binary with spins parallel (*i.e.,* aligned or anti-aligned) to the orbital angular momentum $\boldsymbol{L}$, and denote the masses by $M_{1,2}$ (with $q \equiv M_2/M_1 \leq 1$) and the spin projections on the angular-momentum direction by $S_{1,2} \equiv a_{1,2}\, M_{1,2}^2$ ($a_{1,2}$ being the dimensionless spin-parameter projections). In the EMRL $q \ll 1$, the final-spin projection on the angular-momentum direction must be

$$a_{\rm fin} = a_1 + \nu \left(L_{\rm ISCO}(a_1) - 2a_1 E_{\rm ISCO}(a_1)\right) + \mathcal{O}(\nu^2)\,, \quad (1)$$

with $\nu \equiv q/(1+q)^2$ the symmetric mass ratio, and $L_{\rm ISCO}(a)$, $E_{\rm ISCO}(a)$, respectively the specific (dimensionless) angular momentum and energy for a test particle at the innermost stable circular orbit (ISCO) of a Kerr BH with spin parameter a (Bardeen et al. 1972)

$$E_{\rm ISCO}(a) = \sqrt{1 - \frac{2}{3 r_{\rm ISCO}(a)}}\,, \quad (2)$$

$$L_{\rm ISCO}(a) = \frac{2}{3\sqrt{3}} \left[1 + 2\sqrt{3 r_{\rm ISCO}(a) - 2}\right]\,, \quad (3)$$

$$r_{\rm ISCO}(a) = 3 + Z_2 - \frac{a}{|a|}\sqrt{(3-Z_1)(3+Z_1+2Z_2)}\,, \quad (4)$$

$$Z_1 = 1 + (1-a^2)^{1/3}\left[(1+a)^{1/3} + (1-a)^{1/3}\right]\,, \quad (5)$$

$$Z_2 = \sqrt{3a^2 + Z_1^2}\,. \quad (6)$$

[5] Note that for the simulations of Zlochower & Lousto (2015), we only consider the horizon-extracted data, and *not* the radiation-based ones, which may be imprecise (Lousto private comm. 2016).

The final-spin expression of Rezzolla et al. (2008c) and Barausse & Rezzolla (2009) reproduces Eq. (1) only in the special case $a_1 = 0$, when $a_{\rm fin} = 2\sqrt{3}\nu + \mathcal{O}(\nu^2)$. Indeed, one of the drawbacks of those early expressions is that they may yield spins $a_{\rm fin} > 1$ for small mass ratios $\nu \ll 1$, in clear disagreement with Eq. (1), which predicts $a_{\rm fin} \leq 1$, the equality holding for $a_1 = 1$.

To enforce the EMRL exactly, we consider the following ansatz for the final-spin projection:

$$a_{\rm fin} = a_{\rm tot} + \nu[L_{\rm ISCO}(a_{\rm eff}) - 2a_{\rm tot}(E_{\rm ISCO}(a_{\rm eff}) - 1)] + \sum_{i=0}^{n_M}\sum_{j=0}^{n_J} k_{ij}\nu^{2+i}\, a_{\rm eff}^j\,, \quad (7)$$

where k_{ij} are free coefficients to be determined from the NR data, $a_{\rm tot} \equiv (S_1+S_2)/(M_1+M_2)^2 = (a_1 + a_2 q^2)/(1+q)^2$ is the "total" spin parameter used in Barausse et al. (2012), while $a_{\rm eff} \equiv S_{\rm eff}/(M_1+M_2)^2$ is an "effective" spin parameter. In more detail, we assume $S_{\rm eff} = (1+\xi M_2/M_1)S_1 + (1+\xi M_1/M_2)S_2$, which yields $a_{\rm eff} = a_{\rm tot} + \xi\nu(a_1+a_2)$. This choice is inspired by Damour (2001), who finds that the leading-order conservative spin-orbit dynamics depends on the spin only through $S_{\rm eff}$ with $\xi = 3/4$, while the leading-order conservative spin-spin dynamics depends on $S_{\rm eff}$ with $\xi = 1$ (see also Racine 2008; Kesden et al. 2015; Gerosa et al. 2015). In the following, we will keep ξ as a free parameter and determine it from the NR simulations.[6]

Note that Eq. (7) matches Eq. (1) for $\nu \ll 1$, since $a_{\rm tot} = a_1(1-2\nu) + \mathcal{O}(\nu^2)$. Moreover, by singling out $a_{\rm tot}$ as the first term in Eq. (7), we have isolated the "direct" contribution of the progenitor spins to the remnant's spin. However, this does not mean that all leading-order effects of the smaller BH's spin a_2 are already included. For instance, the specific energy and angular momentum at the ISCO receive corrections of $\mathcal{O}(a_2\,\nu)$ (see *e.g.,* Barausse & Buonanno 2010), which propagate into a term of $\mathcal{O}(a_2\,\nu^2)$ in the final spin, c.f. Eq. (1). This effect, together with other ones, is captured by the coefficient k_{01}.

The coefficients k_{0j} of the ν^2 terms in Eq. (7) also encode the information about the self-force dynamics (both dissipative and conservative) and the leading-order (in mass ratio) plunge-merger-ringdown emission. More specifically, the conservative self-force produces shifts $\nu\,\Delta E_{\rm ISCO}$ and $\nu\,\Delta L_{\rm ISCO}$ in the ISCO specific energy and angular momentum away from the geodesic values of Eqs. (2) and (3). For a nonspinning binary ($a_1 = a_2 = 0$) with $\nu \ll 1$

$$\Delta L_{\rm ISCO} \approx -0.802\,. \quad (8)$$

This follows from evaluating Eq. (3c) of Le Tiec et al. (2012) at the ISCO frequency, which should include conservative self-force effects as in Eq. (5) of the same reference. The plunge-merger-ringdown angular-momentum flux is instead given by (Bernuzzi & Nagar 2010)

$$\Delta J_{\rm MR} \approx 3.46\,\nu^2\,. \quad (9)$$

[6] Setting $\xi = 3/4$ or $\xi = 1$ yields a much larger reduced χ^2 (see below for how we compute it). For $n_M = 1$, $n_J = 2$ ($n_M = 3$, $n_J = 4$) we obtain $\chi^2_{\rm red} \approx 5$ (1.4) for $\xi = 3/4$, and $\chi^2_{\rm red} \approx 51$ (10) for $\xi = 1$. This strong statistical evidence that $\xi \neq 3/4, 1$ is not surprising, as one indeed expects the leading-order spin-orbit and spin-spin couplings to be "deformed" for highly relativistic binaries (Barausse & Buonanno 2010).

k_{01}	k_{02}	k_{10}	k_{11}	k_{12}	ξ
-1.2019	-1.20764	3.79245	1.18385	4.90494	0.41616

k_{01}	k_{02}	k_{03}	k_{10}	k_{11}	k_{12}
2.87025	-1.53315	-3.78893	32.9127	-62.9901	10.0068
k_{13}	k_{20}	k_{21}	k_{22}	k_{23}	k_{30}
56.1926	-136.832	329.32	-13.2034	-252.27	210.075
k_{31}	k_{32}	k_{33}	ξ		
-545.35	-3.97509	368.405	0.463926		

k_{01}	k_{02}	k_{03}	k_{04}	k_{10}	k_{11}
3.39221	4.48865	-5.77101	-13.0459	35.1278	-72.9336
k_{12}	k_{13}	k_{14}	k_{20}	k_{21}	k_{22}
-86.0036	93.7371	200.975	-146.822	387.184	447.009
k_{23}	k_{24}	k_{30}	k_{31}	k_{32}	k_{33}
-467.383	-884.339	223.911	-648.502	-697.177	753.738
k_{34}	ξ				
1166.89	0.474046				

Table 1
The coefficients of our formula, for $n_M = 1,\ n_J = 2$ (top block), $n_M = 3,\ n_J = 3$ (middle block) and $n_M = 3,\ n_J = 4$ (bottom block).

Therefore, for a nonspinning binary one expects

$$\begin{aligned} a_{\rm fin} &\approx \nu L_{\rm ISCO}(0) - 2\nu^2[E_{\rm ISCO}(0)-1]L_{\rm ISCO}(0) \\ &\quad + \Delta L_{\rm ISCO}\nu^2 - \Delta J_{\rm MR} + \mathcal{O}(\nu^3) \\ &\approx 2\sqrt{3}\nu - 3.87\,\nu^2 + \mathcal{O}(\nu^3)\,, \end{aligned} \tag{10}$$

hence $k_{00} \approx -3.87$. (Note that at $\mathcal{O}(\nu)$ and after setting $a_1 = a_2 = 0$, this equation reduces to Eq. (1).) However, since the transition from inspiral to plunge does not happen exactly at the ISCO when accounting for deviations from adiabaticity, but takes place smoothly around the ISCO (Ori & Thorne 2000), and since the the plunge-merger-ringdown fluxes are intrinsically approximate (as it is difficult to define unambiguously the plunge-merger-ringdown as separate from the late inspiral), we keep k_{00} as a free parameter. As it happens, at least for $n_M = 1,\ n_J = 2$, the fitted value is $k_{00} \approx -3.82$, which is reasonably close to the one predicted by the considerations above[7].

In principle, we could fit all the coefficients k_{ij} (as well as ξ) to the NR results. However, since simulations for equal-mass non-spinning BH binaries have determined the final remnant's spin with accuracy far better than for other configurations, we impose that Eq. (7) with $q = 1$ and $a_1 = a_2 = 0$ yields exactly the final spin $a_{\rm fin} = 0.68646 \pm 0.00004$ measured by the NR simulations of Scheel et al. (2009). This gives the relation

$$\frac{\sqrt{3}}{2} + \sum_{i=0}^{n_M} \frac{k_{i0}}{4^{2+i}} = 0.68646 \pm 0.00004\,. \tag{11}$$

With this constraint, we fit Eq. (7) to the 246 simulations for parallel-spin binaries in our calibration dataset.

However, before performing the fit, it is useful to quantify the average error of the final spins calculated from NR simulations. This is possible because our calibration dataset contains simulations by different groups with the same initial data. More precisely, 71 parallel-spin simulations have one or more "twins", *i.e.,* binaries with exactly the same initial properties, so that the *mean* of the absolute differences between twin NR simulations can be measured to be $\delta a_{\rm fin} \approx 0.002$. This estimate allows not only performing a fit, but also computing its reduced chi-squared $\chi^2_{\rm red}$, thus gauging whether we are overfitting the data, which would correspond to $\chi^2_{\rm red} < 1$.

[7] For the cases $n_M = 3, n_J = 3$ and $n_M = 3, n_J = 4$, also considered in the following, $k_{00} \approx -5.9$. However, we will show that unlike $n_M = 1$, $n_J = 2$, those cases are probably overfitting the data.

Model	coeffs.	μ	σ	$\chi^2_{\rm red}$
$n_M = 1,\ n_J = 2$	6	-0.000215	0.00198	0.985
$n_M = 3,\ n_J = 3$	16	-0.000066	0.00168	0.712
$n_M = 3,\ n_J = 4$	20	-0.000029	0.00166	0.694
Barausse & Rezzolla (2009)	4	-0.002310	0.00564	9.313
Husa et al. (2016)	11	-0.000240	0.00453	5.150
Healy et al. (2014)	19	0.000014	0.00170	0.718

Table 2
The mean and rms (μ and σ) of the residuals $a^{\rm num}_{\rm fin} - a^{\rm fit}_{\rm fin}$ from the numerical data, as well as $\chi^2_{\rm red}$, for our formula and those of Barausse & Rezzolla (2009), Husa et al (2016), and Healy et al. (2014); also displayed is the number of coefficients in the various cases.

Since Eq. (7) can be expanded to arbitrary order via its last term, we have performed fits of the parallel-spin calibration dataset with $n_M = 1,\ n_J = 2$ (6 coefficients), $n_M = 3,\ n_J = 3$ (16 coefficients) and $n_M = 3,\ n_J = 4$ (20 coefficients). The fitted coefficients are given in Table 1. Table 2 reports the mean (μ) and root-mean-square (rms, σ) of the residuals from the NR data, as well as $\chi^2_{\rm red}$, for the three aforementioned sets of coefficients, and for the formulae of Barausse & Rezzolla (2009), Husa et al (2016) and Healy et al. (2014) (which use 4, 11 and 19 coefficients, respectively). Table 2 shows that our new formula converges when increasing the number of coefficients, although the optimal choice to avoid overfitting appears to be $n_M = 1,\ n_J = 2$. The convergence of our formula is also displayed in the left panel of Fig. 1, which shows the probability distribution functions (PDFs) of the residuals, obtained as Gaussian fits. The right panel shows instead the (fitted) PDFs for our formula (for $n_M = 3,\ n_J = 4$) and for the formulae of Barausse & Rezzolla (2009), Husa et al (2016) and Healy et al. (2014); the inset shows the actual residual distribution for our formula. Note that already with 16 coefficients our new formula has a slightly smaller rms than Healy et al. (2014), with the important advantage that it can be used also for generic binaries (see below), unlike the formulae of Husa et al (2016) and Healy et al. (2014).

To generalize Eq. (7) to generic spins, we write the remnant's spin as the total spin $\boldsymbol{S} = \boldsymbol{S}_1 + \boldsymbol{S}_2$ plus an angular momentum contribution (*i.e.,* the angular momentum at the binary's "effective" ISCO), *i.e.,* $\boldsymbol{S}_{\rm fin} = \boldsymbol{S} + \Delta\boldsymbol{L}$. Since the final mass is $M_{\rm fin} = (M_1 + M_2)(1 - E_{\rm rad})$ (with $E_{\rm rad} \lesssim 0.1$ the mass radiated in GWs; Barausse et al. 2012), the final spin parameter is

$$\boldsymbol{a}_{\rm fin} = \boldsymbol{a}_{\rm tot} + \boldsymbol{\ell}\nu\,, \quad \boldsymbol{a}_{\rm tot} = \frac{1}{(1+q)^2}\left(\boldsymbol{a}_1 + \boldsymbol{a}_2 q^2\right)\,, \tag{12}$$

where we have reabsorbed the radiated energy $E_{\rm rad}$ in $\boldsymbol{\ell} \equiv \Delta\boldsymbol{L}/[M_1M_2(1-E_{\rm rad})^2] + \boldsymbol{S}[2E_{\rm rad} + 3E^2_{\rm rad} + \mathcal{O}(E_{\rm rad})^3]/(M_1M_2)$ (note that $\boldsymbol{\ell}$ remains finite in the test-particle limit because $|\Delta\boldsymbol{L}| = \mathcal{O}(\nu) = E_{\rm rad}$ as $\nu \to 0$). By evaluating Eq. (12) for parallel spins and comparing it to (7),

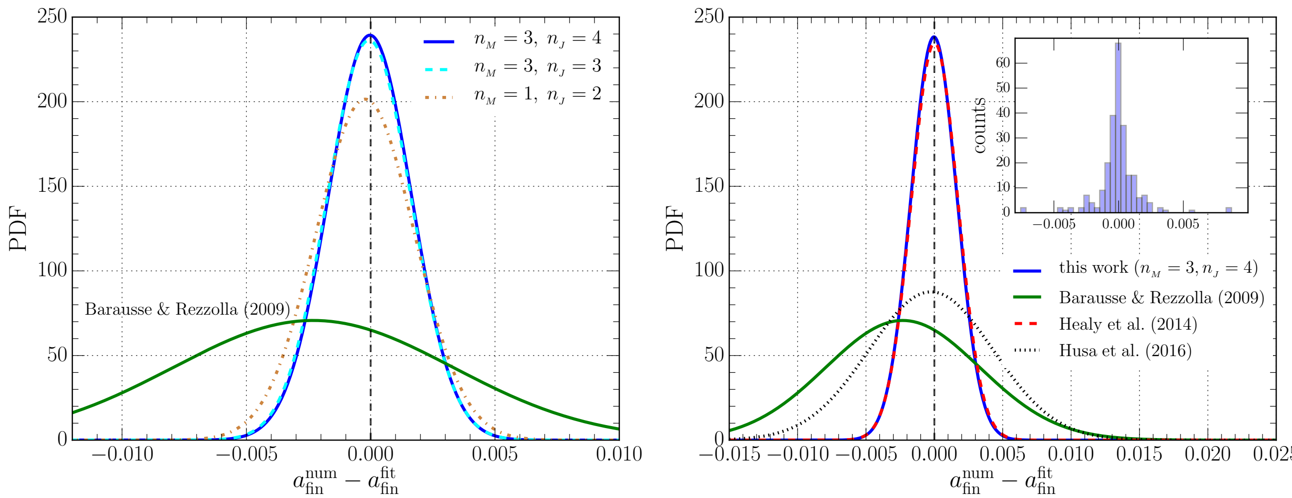

Figure 1. Left panel: probability distribution functions (PDFs), obtained as Gaussian fits, for the residuals of our formula with increasing number of coefficients (*i.e.,* $n_M = 1$, $n_J = 2$; $n_M = 3$, $n_J = 3$; $n_M = 3$, $n_J = 4$) and for that of Barausse & Rezzolla (2009). Right panel: same as the left panel, but for our formula with $n_M = 3$, $n_J = 4$ and for the formulae of Barausse & Rezzolla (2009), Healy et al. (2014), and Husa et al (2016); the inset shows the actual distribution for our formula.

we obtain

$$|\boldsymbol{\ell}| = \Bigg| L_{\rm ISCO}(a_{\rm eff}) - 2a_{\rm tot}\left(E_{\rm ISCO}(a_{\rm eff}) - 1\right) + \sum_{i=0}^{n_M}\sum_{j=0}^{n_S} k_{ij}\nu^{1+i}\, a_{\rm eff}^{j}\Bigg|, \quad (13)$$

which can be generalized to precessing spins by following Barausse et al. (2012) (see also Rezzolla et al. 2008c; Barausse & Rezzolla 2009) and replacing

$$a_{\rm tot} \to a_{\rm tot}(\beta,\gamma,q) \equiv \frac{|\boldsymbol{a}_1|\cos\beta + |\boldsymbol{a}_2|\cos\gamma\, q^2}{(1+q)^2}\,, \quad (14)$$

$$a_{\rm eff} \to a_{\rm eff}(\beta,\gamma,q) \equiv a_{\rm tot}(\beta,\gamma) + \xi\nu(a_1\cos\beta + a_2\cos\gamma)\,, \quad (15)$$

with β (γ) being the angle between $\boldsymbol{a}_1$ ($\boldsymbol{a}_2$) and the orbital angular momentum. Clearly, with this choice Eq. (12) matches Eq. (7) for parallel spins (*i.e.,* for $\beta = 0, \pi$ and $\gamma = 0, \pi$).

Moreover, for equal masses ($q = 1$), the leading-order PN spin effects in the conservative sector (*i.e.,* the leading-order spin-orbit coupling) enter the dynamics only through the combination $\hat{\boldsymbol{L}} \cdot \boldsymbol{S}/M^2 = a_{\rm tot}(\beta,\gamma,1) \propto a_{\rm eff}(\beta,\gamma,1)$ (see *e.g.,* Damour 2001; Barausse & Buonanno 2010), where a "hat" denotes a unit-norm vector. Therefore, at this approximation order, the binding energy and angular momentum at the effective ISCO depend on the spins only through $a_{\rm tot}(\beta,\gamma,1)$ (or equivalently $a_{\rm eff}(\beta,\gamma,1)$), as reflected in Eqs. (13)–(15). Similarly, in the EMRL, the leading contributions to $|\boldsymbol{\ell}|$ come from the ISCO energy and angular momentum of a test particle in Kerr. By construction, $|\boldsymbol{\ell}|$ has the correct EMRL for parallel spins, but the EMRL is also recovered approximately for generic-spin configurations, at least at leading order in the primary-BH spin. Indeed, this happens because the ISCO angular momentum and energy for a test particle in a non-equatorial orbit in a Kerr spacetime are $L_{\rm ISCO}(a_{\rm tot}(\beta,\gamma,0))$ and $E_{\rm ISCO}(a_{\rm tot}(\beta,\gamma,0))$, at leading order in the spin (see discussion in Barausse et al. 2012).

Putting things together, the final-spin magnitude reads

$$|\boldsymbol{a}_{\rm fin}| = \frac{1}{(1+q)^2}\Big[|\boldsymbol{a}_1|^2 + |\boldsymbol{a}_2|^2 q^4 + 2|\boldsymbol{a}_1||\boldsymbol{a}_2|q^2\cos\alpha + 2\left(|\boldsymbol{a}_1|\cos\beta + |\boldsymbol{a}_2|q^2\cos\gamma\right)|\boldsymbol{\ell}|q + |\boldsymbol{\ell}|^2 q^2\Big]^{1/2}, \quad (16)$$

where α is the angle between the two spins. In principle, the angles α, β and γ depend on the binary separation. However, β and γ enter in our formulae only through $a_{\rm tot}(\beta,\gamma,q)$ and $a_{\rm eff}(\beta,\gamma,q)$. These combinations remain constant during the adiabatic inspiral (Apostolatos et al. 1994), if only the leading PN order in the spins (*i.e.,* the leading-order spin-orbit coupling) is included, and either *(i)* the masses are equal; or *(ii)* only one BH is spinning; or *(iii)* the mass ratio is extreme (*i.e.,* $\nu \approx 0$). Similarly, under the same assumptions, we can safely assume that α remains constant during the adiabatic inspiral (Apostolatos et al. 1994), *i.e.,* the angle between the two spins is preserved by the leading-order spin-orbit coupling for equal masses, while it does enter the final-spin prediction if only one BH is spinning, or when $\nu \approx 0$ (indeed, the effect of the smaller BH's spin vanishes at leading order in ν, because $|\boldsymbol{S}_2| = \mathcal{O}(\nu)^2$). Outside these special cases, α, β and γ are not exactly constant. For instance, in general α oscillates and the oscillations may even become "flip-flop"-unstable between separations $r_{\rm ud\pm} = (\sqrt{a_1} \pm \sqrt{q\, a_2})^4 (M_1 + M_2)/(1-q)^2$ for certain unequal-mass configurations where the primary-BH spin is aligned with the orbital angular momentum and the spin of the secondary is anti-aligned with it (Lousto & Healy 2016; Gerosa et al. 2015). These configurations, however, are unlikely if the spins are isotropically distributed, or if the spins are almost aligned with the angular momentum of a circumbinary disk due to the Bardeen-Petterson effect (Bardeen & Petterson 1975).

Therefore, we follow Barausse et al. (2012); Barausse & Rezzolla (2009); Rezzolla et al. (2008c) and define α, β and γ at the initial binary separation $r_{\rm in}$

$$\begin{aligned}\cos\alpha &\equiv \hat{\boldsymbol{a}}_1 \cdot \hat{\boldsymbol{a}}_2|_{r_{\rm in}}\,,\\ \cos\beta &\equiv \hat{\boldsymbol{L}} \cdot \hat{\boldsymbol{a}}_1|_{r_{\rm in}}\,,\\ \cos\gamma &\equiv \hat{\boldsymbol{L}} \cdot \hat{\boldsymbol{a}}_2|_{r_{\rm in}}\,.\end{aligned} \quad (17)$$

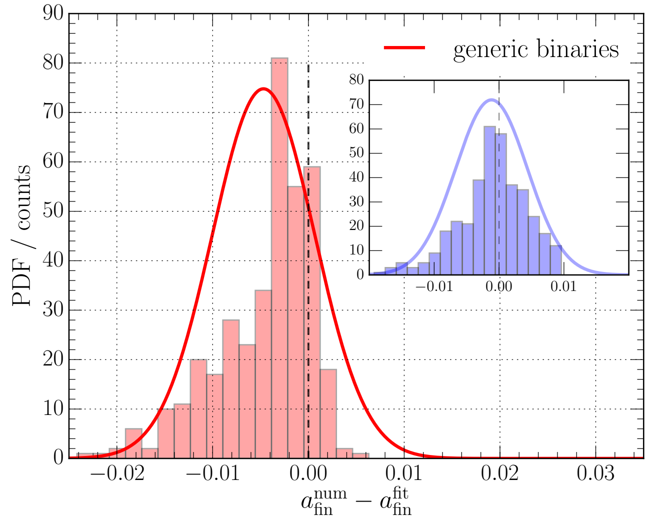

Figure 2. The residual distribution for the remnant spin magnitude, for binaries with generic spins; the inset shows how the modest bias of the distribution can be reduced by adjusting the angles β, γ.

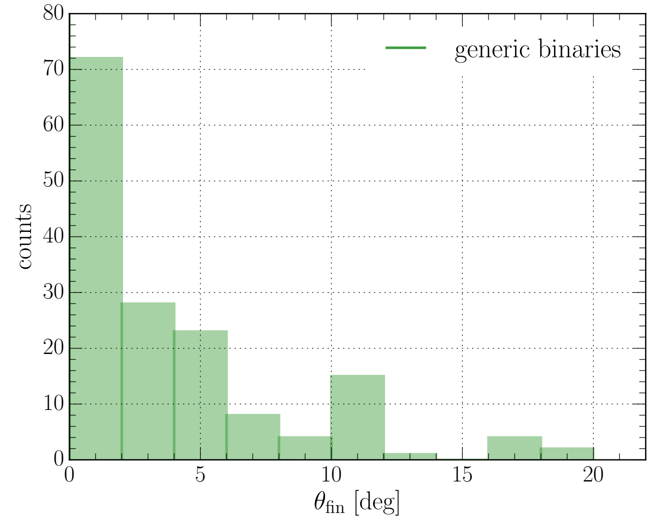

Figure 3. The distribution of the angle between the final spin and the initial direction of the total angular momentum.

Indeed, Barausse & Rezzolla (2009) and Kesden et al. (2010) have verified that the final-spin predictions are robust against the initial separation $r_{\rm in}$, *i.e.,* in most cases the definitions (17) are justified.

A comparison between our new formula with $n_J = 2$, $n_M = 1$ and the generic-spin simulations in our calibration dataset yields the residuals displayed in Fig. 2. Also shown is the corresponding PDF with mean $\mu \approx -0.005$ and rms $\sigma \approx 0.007$. Note that in this case we cannot reliably estimate $\chi^2_{\rm red}$, as none of the generic-spin configurations have "twins" in our calibration dataset, and the NR error is expected to be larger than in parallel-spin binaries because of precession. Also shown by Fig. 2 is an unattractive feature of our formula, namely, that the distribution of residuals is biased toward negative values (*i.e.,* our formula systematically overpredicts the final spin for generic binaries). Although this bias is small, and because it follows from assuming that α, β, γ are constant, we can amend it by replacing the angles α, β, γ by "effective" angles α^*, β^*, γ^* defined as

$$\Theta^* \equiv 2 \arctan\left[(1+\epsilon_\Theta)\tan\frac{\Theta}{2}\right] \approx \Theta + \epsilon_\Theta \sin\Theta\,, \quad (18)$$

where $\Theta = \alpha$, β, γ, ϵ_Θ are free coefficients to be fixed by the data, and we impose $\epsilon_\beta = \epsilon_\gamma$ to make our formula symmetric under exchange of the two BHs. Clearly, for parallel spins $\alpha^* = \alpha$, $\beta^* = \beta$ and $\gamma^* = \gamma$. A comparison with the NR data gives $\epsilon_\alpha \approx 0$ and $\epsilon_\beta = \epsilon_\gamma \approx 0.024$, where we have used the second equality of Eq. (18) (the first equality gives similar results). The corresponding residual distribution has a smaller bias and is shown in the inset of Fig. 2, together with a PDF with $\mu \approx -0.001$, $\sigma \approx 0.006$.

As a further "blind" test of our formula, we consider data from the recently published catalogue of Karan et al. (2016) that is *not* already included in our calibration dataset (*i.e.,* 83 parallel-spin and 165 precessing-spin simulations). Already when using only $n_M = 1$ and $n_J = 2$, the comparison yields mean and rms residuals $\mu \approx -5 \times 10^{-5}$ and $\sigma \approx 1.4 \times 10^{-4}$ for parallel spins, and $\mu \approx -0.004$ ($\mu \approx -0.0005$), and $\sigma \approx 3.3 \times 10^{-4}$ ($\sigma \approx 3.5 \times 10^{-4}$) for precessing spins with unadjusted (adjusted) angles β, γ.

Finally, for the final-spin direction we follow Barausse & Rezzolla (2009); Apostolatos et al. (1994) and note that at leading PN order in the spins (*i.e.,* including the leading-order spin-orbit coupling alone), the GW-driven evolution in the adiabatic inspiral approximately preserves the direction of the total angular momentum $\boldsymbol{J} \equiv \boldsymbol{L} + \boldsymbol{S}$. Barausse & Rezzolla (2009), and later Lousto & Zlochower (2014), verified that $\hat{\boldsymbol{J}}$ is approximately preserved (to within a few degrees) also in the plunge, merger and ringdown. The only exception to this "simple-precession" picture are binaries with spins almost anti-aligned with the orbital angular momentum at large separations (Apostolatos et al. 1994; Kesden et al. 2010). Indeed, when the GW emission sheds enough angular momentum that $\boldsymbol{L} \approx -\boldsymbol{S}$, these binaries undergo "transitional precession" (Apostolatos et al. 1994), whereby the direction of $\hat{\boldsymbol{J}}$ changes significantly on short timescales. Note that among the configurations that give rise to "simple precession" are also the "flip-flop" binaries of Lousto & Healy (2016) and Gerosa et al. (2015). Since transitional-precession configurations comprise a small portion of the parameter space (Kesden et al. 2010), we follow Barausse & Rezzolla (2009) and assume that the final-spin direction is simply given by $\hat{\boldsymbol{J}}(r_{\rm in})$, *i.e.,* the final-spin angle $\theta_{\rm fin}$ relative to the initial angular momentum is simply

$$\cos\theta_{\rm fin} = \hat{\boldsymbol{J}}(r_{\rm in}) \cdot \hat{\boldsymbol{L}}(r_{\rm in})\,. \quad (19)$$

Indeed, the 157 simulations (Zlochower & Lousto 2015; Lousto & Zlochower 2014) in our dataset that report the final-spin direction confirm that the final spin is almost aligned with $\hat{\boldsymbol{J}}(r_{\rm in})$, to within $\sim 18°$ in the worst case, and to within $4°$ ($6°$) in 64% (78%) of the cases. The distribution of the angle between the final spin and $\hat{\boldsymbol{J}}(r_{\rm in})$ is shown in Fig. 3; it is unclear whether the small counts for $\theta_{\rm fin} \gtrsim 10°$ are due to imprecisions in the formula or in the numerical simulations.

Finally, we note that unlike other formulae for the final-spin direction (Buonanno et al. 2008; Tichy & Marronetti 2008; Rezzolla et al. 2008c), Eq. (19) is valid also when $r_{\rm in} \gg M_1 + M_2$. (This is also the case for our formula for the final-spin magnitude.) This is particularly important to predict the final spin in massive BH mergers. Indeed, cosmological simulations (both numerical and semi-analytical ones) cannot follow the evolution of massive BH binaries below the separation $r_{\rm GW}$ at which the GW dynamics starts driving the orbital evolution. For a binary with $M_1 + M_2 \sim 10^8\,M_\odot$ in a gas-poor environment, $r_{\rm GW} \sim 10^{-2}\,{\rm pc} \sim 2\times10^3\,(M_1+M_2)$, a separation at which other prescriptions for the final-spin direction become significantly inaccurate (see discussion in Barausse & Rezzolla 2009; Barausse 2010).[8]

3. CONCLUSION

By combining information from the test-particle limit, perturbative/self-force calculations, the PN dynamics, and an extensive set of NR simulations collected from the literature, we have constructed a novel formula for the final spin from the merger of quasi-circular BH binaries with arbitrary mass ratios and spins. When applied to parallel-spin configurations, our novel formula performs better than other expressions in the literature, and we have also tested its validity for precessing-spin binaries, which other formulae are not able to model accurately. Also, unlike models such as that of Healy et al. (2014), our formula is purely algebraic. Finally, we have used our collected NR dataset to confirm that the final-spin direction is almost parallel to the initial total angular-momentum direction, as first suggested by Barausse & Rezzolla (2009).

We thank Nathan Johnson-McDaniel for useful comments and Davide Gerosa for clarifications on flip-flop binaries. We acknowledge support from the European Union's Seventh Framework Programme (FP7/PEOPLE-2011-CIG) through the Marie Curie Career Integration Grant GALFORMBHS PCIG11-GA-2012-321608, from the H2020-MSCA-RISE-2015 Grant No. StronGrHEP-690904, and from the ERC Synergy Grant "BlackHoleCam - Imaging the Event Horizon of Black Holes" (Grant 610058).

[8] In a gas-rich environment, the separation $r_{\rm GW}$ below which GWs dominate the binary evolution and our formulae can be applied is smaller (Armitage & Natarajan 2012), while for "flip-flop" binaries our formula for the final-spin magnitude might be applicable only below $r_{\rm ud\pm}$.

REFERENCES

Abbott, B. P., et al. 2016, Phys. Rev. Lett., 116, 061102
Ajith, P., et al. 2008, Phys. Rev. D, 77, 104017
Apostolatos, T. A., Cutler, C., Sussman, G. J., & Thorne, K. S. 1994, Phys. Rev. D, 49, 6274
Armitage, P., & Natarajan, P. 2012, Astrophys. J., 567, L9
Barausse, E. 2010, Journal of Physics Conference Series, 228, 012050
Barausse, E. 2012, MNRAS, 423, 2533
Barausse, E., & Buonanno, A. 2010, Phys. Rev., D81, 084024
Barausse, E., Morozova, V., & Rezzolla, L. 2012, Astrophys. J., 758, 63
Barausse, E., & Rezzolla, L. 2009, Astrophys. J. Lett., 704, L40
Bardeen, J. M., & Petterson, J. A. 1975, Astrophys. J., 195, L65
Bardeen, J. M., Press, W. H., & Teukolsky, S. A. 1972, Astrophys. J., 178, 347
Belczynski, K., Buonanno, A., Cantiello, M., et al. 2014, ApJ, 789, 120
Belczynski, K., Repetto, S., Holz, D. E., et al. 2016, ApJ, 819, 108
Bernuzzi, S., & Nagar, A. 2010, Phys. Rev. D, 81, 084056
Berti, E., & Volonteri, M. 2008, ApJ, 684, 822-828
Buchman, L. T., et al. 2012, Phys. Rev. D, 86, 084033
Buonanno, A., & Damour, T. 1999, Phys. Rev., D59, 084006
Buonanno, A., Kidder, L. E., & Lehner, L. 2008, Phys. Rev. D, 77, 026004
Chu, T. et al., 2009, Phys. Rev. D, 80, 124051
Damour, T. 2001, Phys. Rev. D, 64, 124013
Damour, T., & Nagar, A. 2007, Phys. Rev. D, 76, 044003
Dubois, Y., Volonteri, M., & Silk, J. 2014, MNRAS, 440, 1590
Fanidakis, N., Baugh, C. M., Benson, A. J., et al. 2011, MNRAS, 410, 53
Gerosa, D., Kesden, M., O'Shaughnessy, R., et al. 2015, arXiv:1506.09116
Hannam, M., Husa, S., Ohme, F., Mueller, D., & Bruegmann, B. 2010, Phys. Rev. D, 82, 124008
Healy, J., Lousto, C. O., & Zlochower, Y. 2014, Phys. Rev. D, 90, 104004
Hemberger, D. A., et al. 2013, Phys. Rev. D, 88, 064014
Hinder, I., et al. 2013, Classical Quantum Gravity, 31, 025012
Husa, S., et al. 2016, Phys. Rev. D, 93, 044007
Karan, J., et al. 2016, arXiv:1605.03204
Kelly, B. J., et al. 2011, Phys. Rev. D, 84, 084009
Kelly, B. J., & Baker, J. G. 2013, Phys. Rev. D, 87, 084004
Kesden, M. 2008, Phys. Rev. D, 78, 084030
Kesden, M., Sperhake, U., & Berti, E. 2010, Phys. Rev. D, 81, 084054
Kesden, M., Gerosa, D., O'Shaughnessy, R., Berti, E., & Sperhake, U. 2015, Phys. Rev. Lett., 114, 081103
Gerosa, D., Kesden, M., Sperhake, U., Berti, E., & O'Shaughnessy, R. 2015, Phys. Rev. D, 92, 064016
Khan, S., et al. 2015, arXiv:1508.07253
Klein, A., et al. 2016, Phys. Rev., D93, 024003
Le Tiec, A., Barausse, E., & Buonanno, A. 2012, Phys. Rev. Lett., 108, 131103
Lousto, C. O., 2016, private communication.
Lousto, C. O., & Healy, J. 2016, arXiv:1601.05086
Lousto, C. O., & Zlochower, Y. 2014, Phys. Rev. D, 89, 021501
Lousto, C. O., & Zlochower, Y. 2014, Phys. Rev. D, 89, 104052
Lovelace, G., Boyle, M., Scheel, M. A., & Szilágyi, B. 2012, Classical Quantum Gravity, 29, 045003
Lovelace, G., et al. 2015, Classical Quantum Gravity, 32, 065007
Manchester, R. N., & IPTA. 2013, Classical Quantum Gravity, 30, 224010
McClintock, J. E., et al. 2011, Classical Quantum Gravity, 28, 114009
Nakano, H., et al. 2011, Phys. Rev. D, 84, 124006
Ori, A., & Thorne, K. S. 2000, Phys. Rev. D, 62, 124022
Pekowsky, L., O'Shaughnessy, R., Healy, J. & Shoemaker, D. 2013, Phys. Rev. D, 88, 024040
Pollney, D., & Reisswig, C. 2011, Astrophys. J. Lett., 732, L13
Racine, É. 2008, Phys. Rev. D, 78, 044021
Rezzolla, L., Dorband, E. N., Reisswig, C. et al. 2008a, Astrophys. J., Lett. 674, L29
Rezzolla, L., Diener, P., Reisswig, C. et al. 2008b, Astrophys. J., 679, 1442
Rezzolla, L., Barausse, E., Dorband, E. N., et al. 2008c, Phys. Rev., D78, 044002
Scheel, M. A., Boyle, M., Chu T., et al. 2009, Phys. Rev. D, 79, 024003
Scheel, M. A., Giesler, M., Hemberger, D. A., et al. 2015, Classical Quantum Gravity, 32, 105009
Sesana, A., Barausse, E., Dotti, M., & Rossi, E. M. 2014, Astrophys. J., 794, 104
Sperhake, U., Berti, E., & Cardoso, V. 2011, arXiv:1107.2819
SXS collaboration, 2016, www.black-holes.org
Szilágyi, B., Blackman, J., Buonanno, A., et al. 2015, Phys. Rev. Lett., 115, 031102

Tichy, W., & Marronetti, P. 2008, Phys. Rev. D, 78, 081501
Volonteri, M., Sikora, M., Lasota, J.-P., & Merloni, A. 2013, ApJ, 775, 94
Zlochower, Y., & Lousto, C. 2015, Phys. Rev. D, 92, 024022